# A STRUCTURAL AND MORPHOLOGICAL INVESTIGATION OF SUSTAINABLE GREEN ELECTRICITY GENERATION AT AMBIENT TEMPERATURE THROUGH WATER SPLITTING IN A V₂O₅ BASED HYDROELECTRIC CELL

**Thesis submitted**

**In partial fulfilment of the requirements for the**

**Degree of**

## MASTER OF SCIENCE

**in**

**Physics**

**by**

**Archana Krishnan**

**(2K22/MSCPHY/52)**

**Under the supervision of**

**Prof. Nitin K. Puri**

**(Delhi Technological University)**



**To the**

**Department of Applied Physics**

## DELHI TECHNOLOGICAL UNIVERSITY

**(Formerly Delhi College of Engineering)**

**Shahbad Daulatpur, Main Bawana Road, Delhi-110042**

**May,2024**

**DELHI TECHNOLOGICAL UNIVERSITY**
(Formerly Delhi College of Engineering)
Shahbad Daulatpur, Main Bawana Road, Delhi-42

# ACKNOWLEDGEMENTS

**DELHI TECHNOLOGICAL UNIVERSITY**
(Formerly Delhi College of Engineering)
Shahbad Daulatpur, Main Bawana Road, Delhi-42

## CANDIDATE'S DECLARATION

I, **Archana Krishnan (2K22/MSCPHY/52)** student of M.Sc physics, hereby certify that the work which is being presented in the thesis entitled **"A structural and morphological investigation of sustainable green electricity generation at ambient temperature through water splitting in a $V_2O_5$ based hydroelectric cell"** in partial fulfilment of the requirement for the award of the degree of Master in Science, submitted in the Department of Applied Physics, Delhi Technological University is an authentic record of my own work carried out during the period from May 2023 to May 2024 under the supervision of Professor Nitin Kumar Puri.

The matter represented in the thesis has not been submitted by me for the award of any other degree of this or any other institute.

**Archana Krishana**
**(2k22/MSCPHY/52)**

This is to certify that the student has incorporated all the corrections suggested by the examiner in the thesis and the statement made by the candidate is correct to the best of our knowledge.

**Prof. Nitin K. Puri**                                      **Signature of External Examiner**
**(Supervisor)**

**DELHI TECHNOLOGICAL UNIVERSITY**
(Formerly Delhi College of Engineering)
Shahbad Daulatpur, Main Bawana Road, Delhi-42

## CERTIFICATE BY THE SUPERVISOR

Certified that **Archana Krishnan (2k22/MSCPHY/52)** has carried out the search work presented in this thesis entitled "**A structural and morphological investigation of sustainable green electricity generation at ambient temperature through water splitting in a V$_2$O$_5$ based hydroelectric cell**", for the award of **Master of Physics from Department of Applied Physics, Delhi Technological University, Delhi** under my supervision. The thesis embodies result of original work, and studies are carried out by the student herself and the content of the thesis do not form the basis for the award of any other degree to the candidate or to anybody else from this or any other university.

**Prof. Nitin K. Puri**
**(Department of Applied Physics)**
**Delhi Technological University**

# ABSTRACT

Owing to its many benefits, such as high energy density, affordability, availability, and good safety profiles, vanadium-based oxides have attracted much attention. With its comparatively better electrical characteristics, vanadium pentoxide has been the most stable of the several families of vanadium oxides and has been the focus of numerous research for more than 20 years. We have investigated $V_2O_5$ in detail in the current work. We have synthesized the sample using the solid-state sintering technique, starting with pure $V_2O_5$ as a precursor. XRD, FESEM, Raman, FTIR, PL, BET, and Nquist spectroscopy are among the analytical methods that have been used to describe the $V_2O_5$ sample. Structural and phase analyses have been carried out using XRD. The morphological and microstructure have been examined using FESEM. $V_2O_5$ nanoparticles have been found to exhibit rotational, vibrational, and other states by the use of Raman spectroscopy. FTIR identified the bonds. The existence of oxygen vacancies on the surface was verified by PL spectroscopy. The porosity and surface area of the sample have been examined using BET analysis, and the charge transfer mechanism and the ionic current production in the HEC have been investigated using Nyquist and I-V polarization plots. The green energy produced does not discharge poisonous or dangerous materials into the environment. Hence, the current study has proven the manufacture of a $V_2O_5$-based HEC and observed no significant negative environmental impact from the energy produced by $V_2O_5$ HEC.

# LIST OF PUBLICATIONS

**Title of Paper:** Structural and morphological properties of solid-state synthesized $V_2O_5$ nanoparticles for multifunctional applications.

**Author Names:** Archana Krishnan, Hemant K. Arora, Nitin K. Puri

**Name of Conference:** International Conference on Atomic, Molecular, Material, Nano and Optical Physics

**Status of Paper (Accepted/Published/Communicated):** Communicated

# TABLE OF CONTENTS

# LIST OF FIGURES

# LIST OF SYMBOLS AND ABBREVIATIONS

| Symbols | Abbreviations |
| --- | --- |
| & | and |
| $V_2O_5$ | Vanadium pentoxide |
| NPs | Nanoparticles |
| HEC | Hydroelectric cell |
| Zn | Zinc |
| Ag | Silver |
| XRD | X-ray diffraction |
| FESEM | Field emission scanning electron microscopy |
| PL | Photoluminescence |
| FTIR | Fourier transform infrared |
| BET | Brunauer-Emmett-Teller |
| BJH | Barrett-Joyner-Halenda |
| V | Vanadium |
| O | Oxygen |
| DI | Deionized |
| EF | Electric field |
| MOS | Metal oxide semiconductor |
| CVD | Chemical vapour deposition |

| | |
|---|---|
| NRs | Nanorods |
| NWs | Nanowires |
| NSs | Nanospheres |
| EIS | Electrochemical impedance spectroscopy |
| $R_{ct}$ | Charge transfer resistance |
| $R_s$ | Ohmic resistance |
| Z' | Real impedance |
| Z" | Imaginary impedance |
| I-V | Current-voltage |
| $I_{sc}$ | Short circuit current |
| $V_{oc}$ | Open circuit voltage |

# CHAPTER 1

# Introduction

$V_2O_5$, an n-type semiconductor is gaining interest in several ways with $\alpha$-$V_2O_5$ standing out due to its elevated oxygen states [1]. Several polymorphic phases, such as $\alpha$-$V_2O_5$, $\beta$-$V_2O_5$, & $\gamma$-$V_2O_5$, have crystal structures that are orthorhombic, tetragonal, or monoclinic, respectively [2]. To address the challenges associated with $V_2O_5$ electrical characteristics & its applications as a cathode-active material in batteries, a great deal of research has been done [3] [4]. To solve energy difficulties & expedite the transition to sustainable energy systems, it is imperative to investigate a range of energy harvesting techniques, such as hydro, solar, etc. To realize their full potential, these sectors are undergoing intensive investigation [5].

Scientists & researchers have looked into & analyzed a broad range of alternatives throughout the years, including transition metal oxides, sulfides, nitrides, etc [6]. ZnO, CuO, $TiO_2$, $SnO_2$, & $V_2O_5$ are examples of MOS that are widely utilized in gas sensors, batteries, catalysts, & other devices. Because of its great sensitivity, low cost, quick reaction time, & long-term stability, MOS has attracted a lot of attention in gas sensing applications [7]. Vanadium-based oxides have shown to be a promising class of materials among those previously studied. Vanadium is an extremely common element in nature, & since it interacts with oxygen so fast at high temperatures, it is hard to keep it in its metal state. Vanadium's electrical arrangement results in a variety of valence states, which cause oxidation to develop in the oxidation states from $V^{5+}$ to $V^{3-}$ [8]. The crystalline formations & exceptional physical properties of vanadium oxide nanostructures are widely recognized [9]. Vanadium monoxide, vanadium dioxide, vanadium sesquioxide, and vanadium pentoxide, with valences of +2, +3, +4, & +5, respectively, are the most often found oxides that have a single oxidation characteristic [10].

1
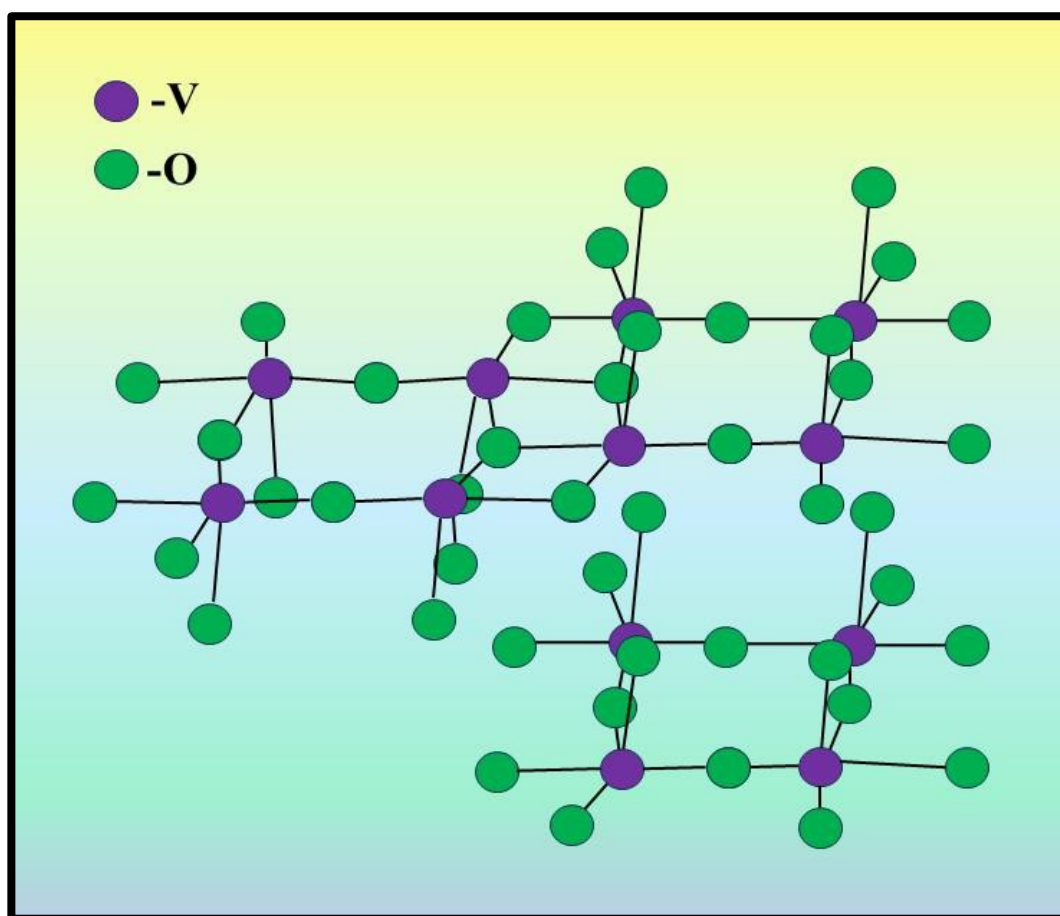
**Figure 1.1 Structure of V$_2$O$_5$**

Moreover, the formation of various oxides such as V$_8$O$_{15}$, V$_7$O$_{13}$, & V$_6$O$_{11}$ (combination of V$^{4+}$ & V$^{3+}$) & mixed valence oxides like V$_6$O$_{13}$ (combination of V$^{5+}$ & V$^{4+}$) is facilitated by oxygen vacancies in the corresponding phase [11]. The primary reason for the increased interest in these materials is the metal-insulator transition seen in vanadium oxides, such as VO, V$_2$O$_3$, VO$_2$, & V$_2$O$_5$ [12]. Significant investigation has been conducted into their potential applications in sensors, electrical switches, & improvements to optical, thermochromic, & electrochemical capabilities as a result of this phenomenon [13-15]. Surprisingly V$_2$O$_3$ is commonly utilized as a catalyst for chemical looping dry reforming of methane, water splitting, and other processes, and it may even find usage in aqueous Zn metal batteries [16]. In the meanwhile, VO$_2$ finds use in temperature sensors, gas sensors, optical photodetectors, & other devices [1].

For the purpose of creating $V_2O_5$ nanostructures, a number of synthesis techniques have been developed, such as hydrothermal, sol-gel, ball milling, CVD, atomic layer deposition, etc. Despite being time-consuming, the solid-state sintering process is the most popular among these methods because of its affordability, ease of use, and environmental friendliness [17]. Many $V_2O_5$ nanostructures such as NPs, NRs, NWs, NSs, etc., have been created & investigated over time. It has been noted that these synthesis methods have demonstrated the critical roles that temperature & synthesis methods play in the formation of various nanostructures [9].

The capabilities of $V_2O_5$ were examined in this work, with a focus on the synthesis technique for nanostructure development. We deliberately selected the solid-state sintering process because it provides a practical & cost-effective way to produce $V_2O_5$ NPs. We can manufacture $V_2O_5$ at a low cost & high production rate with this technology [18]. We improved our grasp of the processed sample's qualities by carefully analyzing their structural & morphological characteristics using several characterizations. After a thorough study, we concluded that this material possesses the ability for energy harvesting applications.

As the depletion of non-renewable resources like oil, wood biomass, & coal due to industrial & population growth is causing a severe energy crisis, green energy alternatives are needed to increase energy production without causing air pollution or carbon dioxide [36]. The most promising technique among others is water-based technology for green electricity production. HEC uses the dissociation of water molecules on the surface to generate electricity by redox process between the Zn anode & Ag cathode [37].
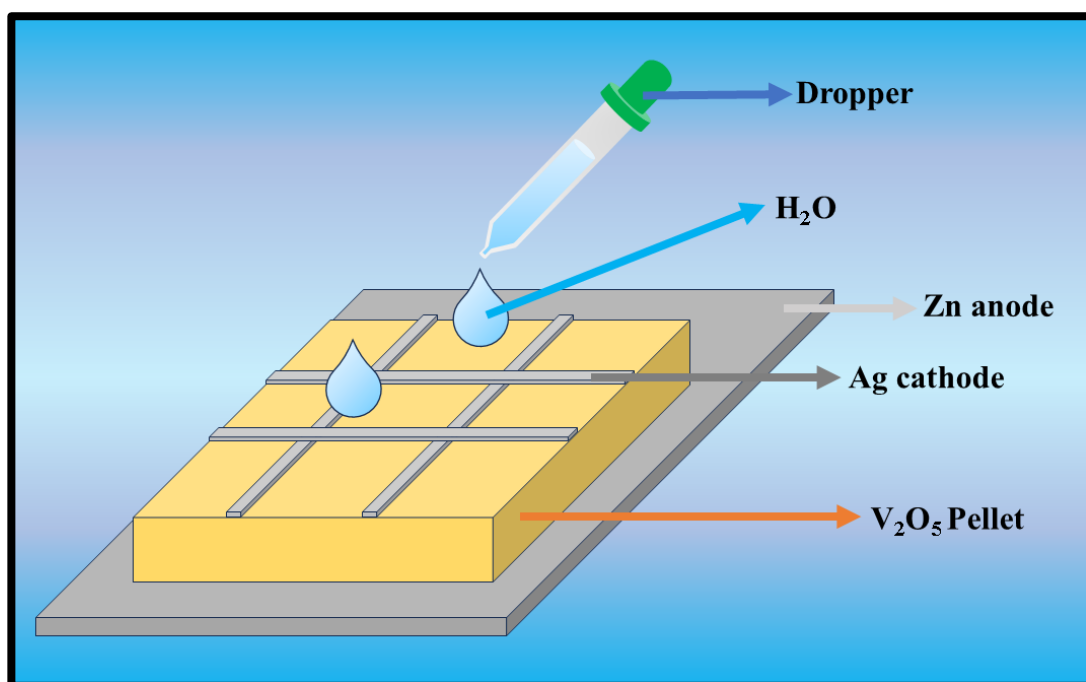
**Figure 1.2 Illustrated diagram of V₂O₅ based Hydroelectric Cell**

This indicates that the green electrical energy created does not discharge poisonous or dangerous materials into the environment. In order to confirm water dissociation at ambient temperature & achieve a notable electrical output, the current study has proven the manufacture of a $V_2O_5$-based HEC by substituting ferrite material and observed no significant negative environmental impact from the energy produced by $V_2O_5$ HEC [38] [39].

# CHAPTER 2

# EXPERIMENTAL SECTION

## 2.1 Material & Method used: -

Vanadium pentoxide of analytical grade (99.6%) was utilized precisely as supplied by Sigma Aldrich.

**Solid State Reaction Method: -**

Solid state synthesis, sometimes referred to as the ceramic technique, is a chemical process that starts with solid materials and ends with the formation of a new solid substance with a predetermined structure. The end products of this method, which include thin-film, polycrystalline materials, glasses, etc, are widely used in the energy and electrical systems domains.

In this process, fine-grain metallic combinations are mixed completely, formed into pellets, and heated to specified temperatures for a certain amount of time. A lot of metallic compounds, including metallic oxides combined with salts, require harsh conditions, like high pressure and temperature, to start operations in a melted flux or a rapidly condensed vapor phase.

In a solid-state process, the evaluation of the reaction rate is crucial. Solid-state processes must finish as there are few ways to purify the resultant solids. In solid-state synthesis, several factors affect the pace of reaction, such as the thermodynamic properties related to nucleation and reactions, as well as the structure, organization, and rate of diffusion. The chemical and physical properties of the final products are largely determined by the chemical precursors and processing methods performed.

## 2.2 Synthesis of $V_2O_5$ powder: -

The solid-state method of synthesis began with the use of pure $V_2O_5$ powder as the precursor, as shown in Figure 2.1. To obtain the ideal fineness, the analytical grade

powder was first carefully grounded for an hour straight with the help of mortar and pestle. The sample was then calcined for two hours at 450 ˚C in a muffle furnace to remove any remaining contaminants. Additionally, five more hours of hand-grinding were used for further refining. The powder was then annealed for five hours at 350 ˚C, and then sintered for two hours at 500˚C in order to further refine its crystal structure and promote the formation of a nanoporous structure. The result of these procedures was the powder that was obtained after sintering, which was the ultimate product.
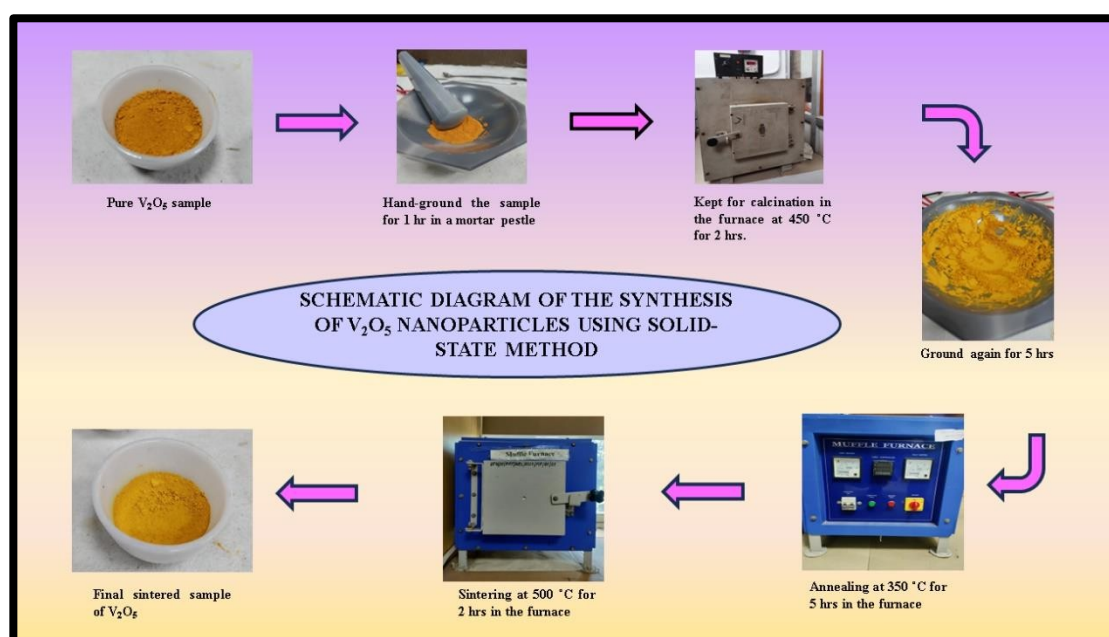


**Figure 2.1 Schematic diagram showing the synthesis process of $V_2O_5$ nanoparticles using solid-state sintering method**

## 2.3 Fabrication of $V_2O_5$ based Hydroelectric Cell: -

Using a hydraulic press machine, the previously synthesized pre-sintered sample was formed into a square pellet with dimensions of $2\times2$ cm$^2$, as shown in Figure 2.2. To create defects in the material, the resulting pellet was sintered for two hours at 500 ˚C to harden it. Defects were made on the surface of this oxygen-deficient square pellet to facilitate the advantageous dissociation of water molecules. On both sides of the pellet, electrodes consisting of Zn as the anode and Ag as the cathode were constructed. Zn sheets were adhered to the other side of the pellet for hydroelectric

characterization, and conducting Ag paint was applied in a grid-like pattern. In the end, to create a completely functional HEC, an electrical connection was made to the pellet.
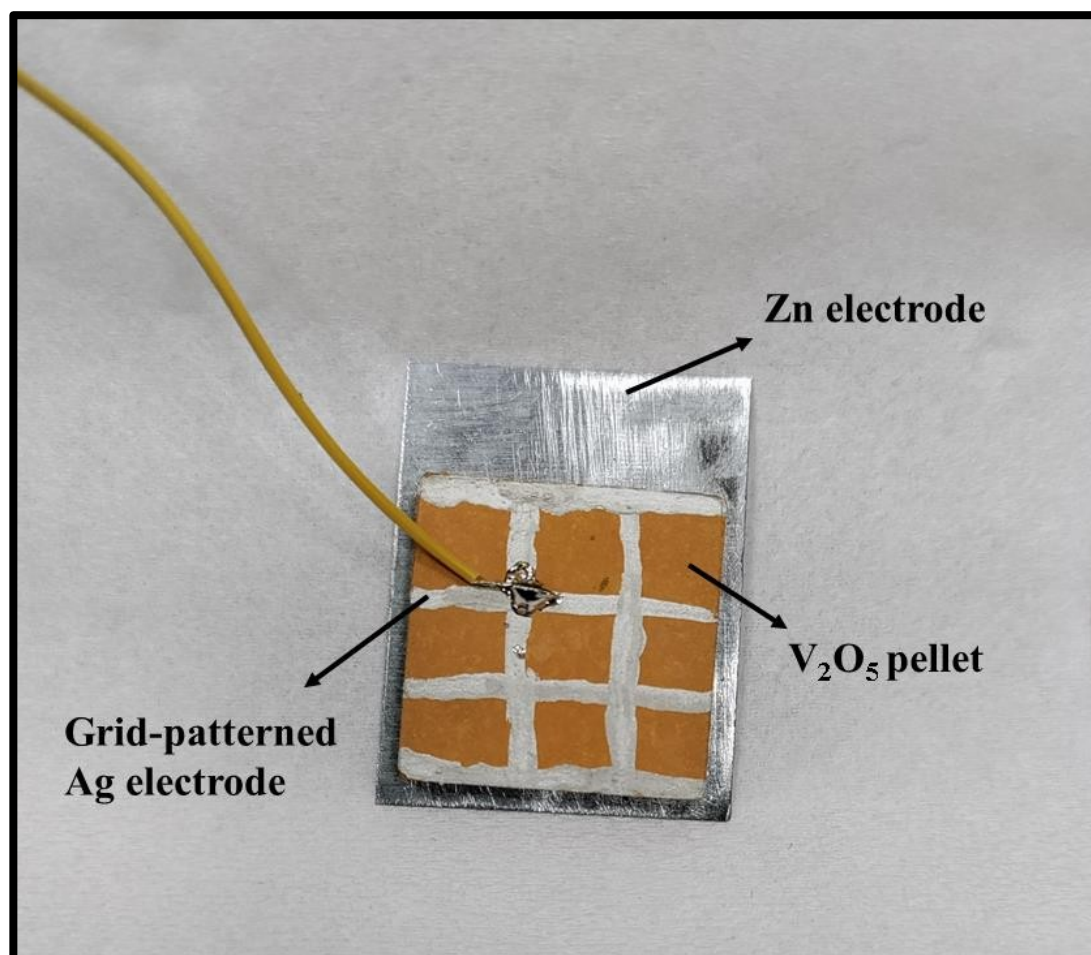


**Figure 2.2 Image of fabricated hydroelectric cell**

## 2.4 Characterization Techniques: -

The generated $V_2O_5$ powders were analyzed within the 10˚–80˚ range using a Bruker D8 X-ray diffractometer configured with Cu–Kα radiation at a wavelength of 0.154nm. XRD was used to investigate the crystal structure of the sample.

**Figure 2.3 Cu-Kα radiation, λ= 1.5406 Å, Make Bruker, Model: D8 Discover**

Using field emission scanning electron microscopy (FESEM, JEOL JSM-6610LV) at an accelerating voltage of 10 kV, surface morphology was examined. Raman spectroscopy using a photoluminescence spectrometer and a diode laser to provide a fixed excitation wavelength of 325 nm, photoluminescence measurements were carried out.

**Figure 2.4 Photograph of JEOL Japan Mode: JSM 6610LV SEM**

Furthermore, data from Fourier transform infrared spectroscopy was obtained for the specimen. The Brunauer-Emmett-Teller nitrogen adsorption isotherm (Quanta chrome instrument, Nova 2000e) was used to determine the pore's specific surface area, volume, size, & other relevant parameters for the $V_2O_5$ sample. The generated HEC of $V_2O_5$ was measured for voltage and current using a digital multimeter. Using a 3-electrode configuration, a bioelectrochemical workstation was utilized to get the Nyquist plots of $V_2O_5$-based HEC.

**Figure 2.5 Photograph of Perkin Elmer Two–Spectrum FTIR spectrometers**

# CHAPTER 3

# Result and Discussion

## 3.1 XRD analysis of $V_2O_5$: -

The XRD measurements as seen in Figure 3.1 verified the sample's crystallinity and structure, showing that the $V_2O_5$ sample had an orthorhombic crystal structure. Bragg peaks were observed at 15.3˚, 20.3˚, 21.6˚, 26.1˚, 30.9˚, 32.2˚, 34.2˚, 41.2˚, 41.8˚, 45.4˚, 47.2˚, 47.7˚, & 51.8˚ in the diffraction pattern, which corresponded to different crystallographic planes, such as (200), (001), (101), (110), (400), (011), (310), (002), (102), (411), (302), & (601). When compared to the standard JCPDS no. 00-041-1426 for $V_2O_5$, the acquired data matched it fairly [19]. Additionally, no more peaks were seen, suggesting that the solid-state method of $V_2O_5$ production was effective.
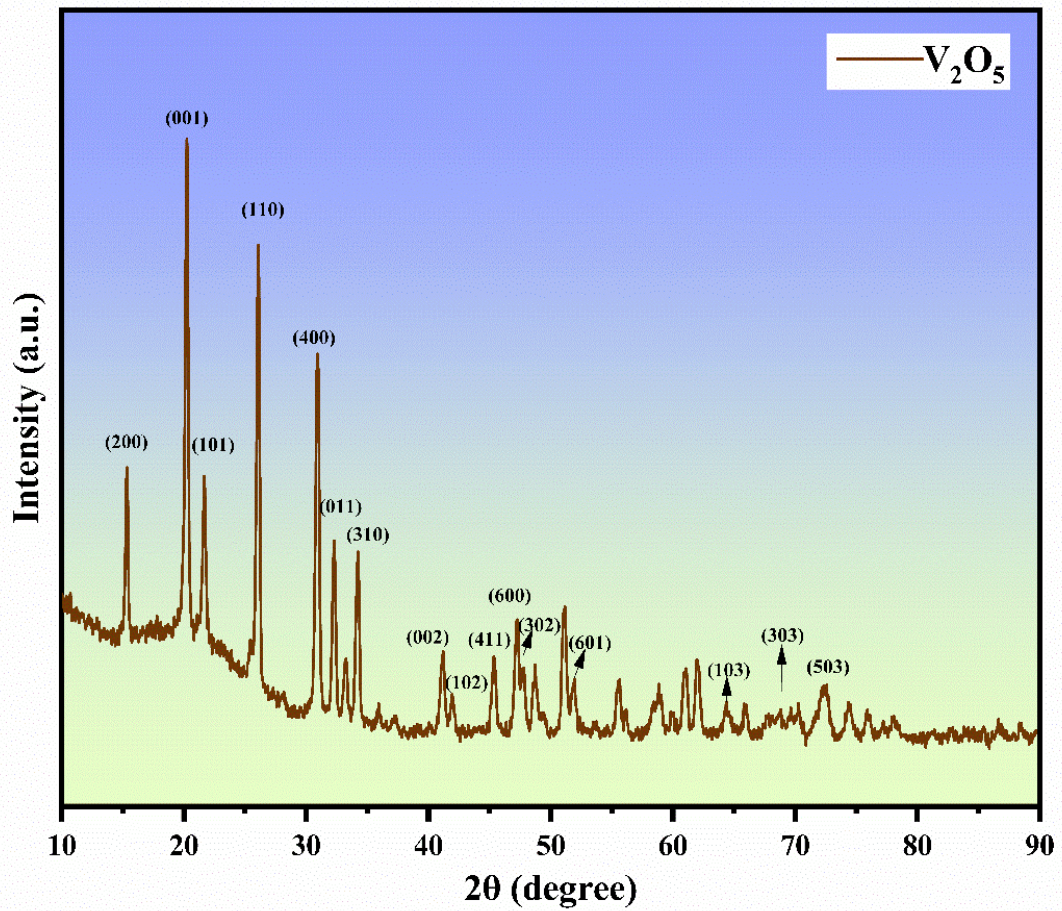
**Figure 3.1 XRD pattern of as-synthesized V$_2$O$_5$ nanoparticles**

The crystallite size was determined utilizing the Debye-Scherrer equation:

$$D = K. \frac{\lambda}{\beta.\cos\theta}$$

where K is the Scherrer constant with a value of 0.9, $\lambda$=0.154 nm is the wavelength of incident radiation, $\beta$ is the full-width half maxima, & $\theta$ is the Bragg's angle. D in the equation represents the material's crystallite size. It was determined that the V$_2$O$_5$ sample's crystallite size was 22.81 nm. In addition, the following equations were used to estimate the strain ($\varepsilon$) & dislocation ($\delta$):

$$\varepsilon = \frac{\beta}{4.\tan\theta}$$

$$\delta = {}^{1}/_{D^2}$$

According to the calculations, the values were 2.05 nm$^{-2}$ for $\delta \times 10^{-3}$ & 5.75 for $\varepsilon \times 10^{-3}$. Figure 3.2 shows the Williamson-Hall plot, which was utilized to validate the estimated lattice strain and crystallite size [20] [21] [22].
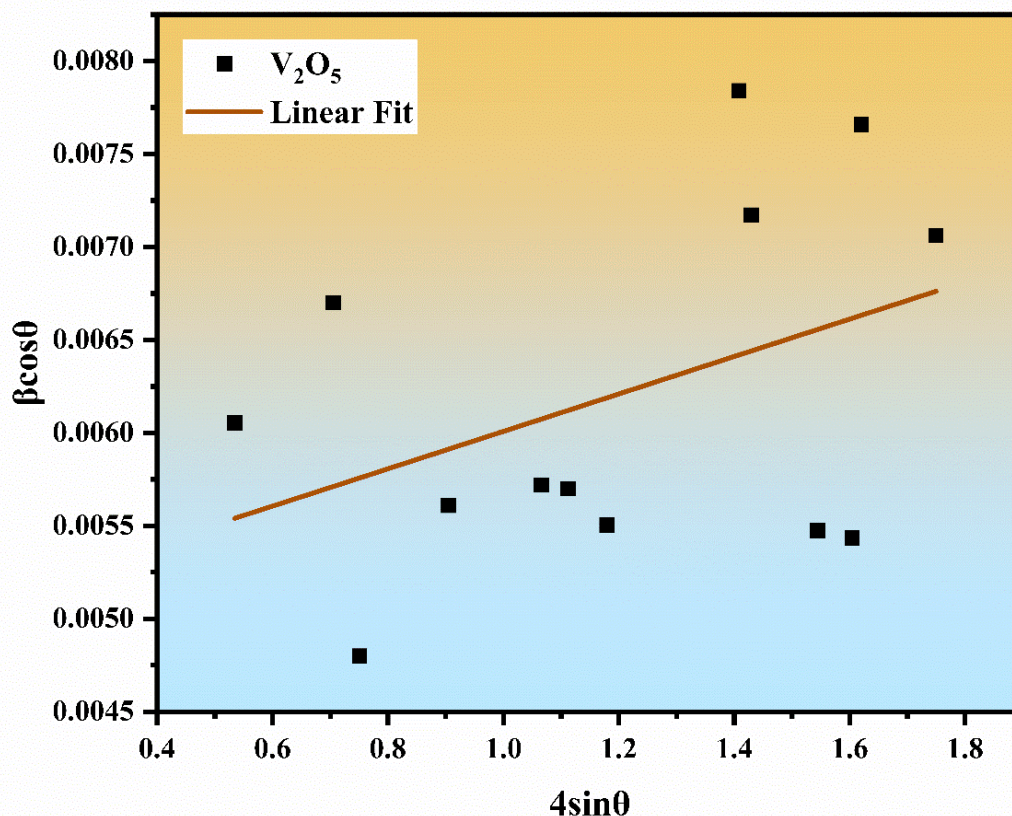


**Figure 3.2 Williamson–Hall (W–H) plot of V₂O₅nanoparticles**

## 3.2 FESEM analysis of $V_2O_5$: -

A thorough look at the surface morphology & porosity of the sample post-synthesis is provided by the FESEM picture shown in Figure 3.3. In addition to being evenly dispersed, tightly packed NPs, it depicts the existence of aggregated grains with large holes [23]. The average diameter of the NPs is 81.6 nm, with a range of 40–90 nm [24]. The complex structure & nanoscale properties of the synthetic $V_2O_5$ material are highlighted by this observation [25].
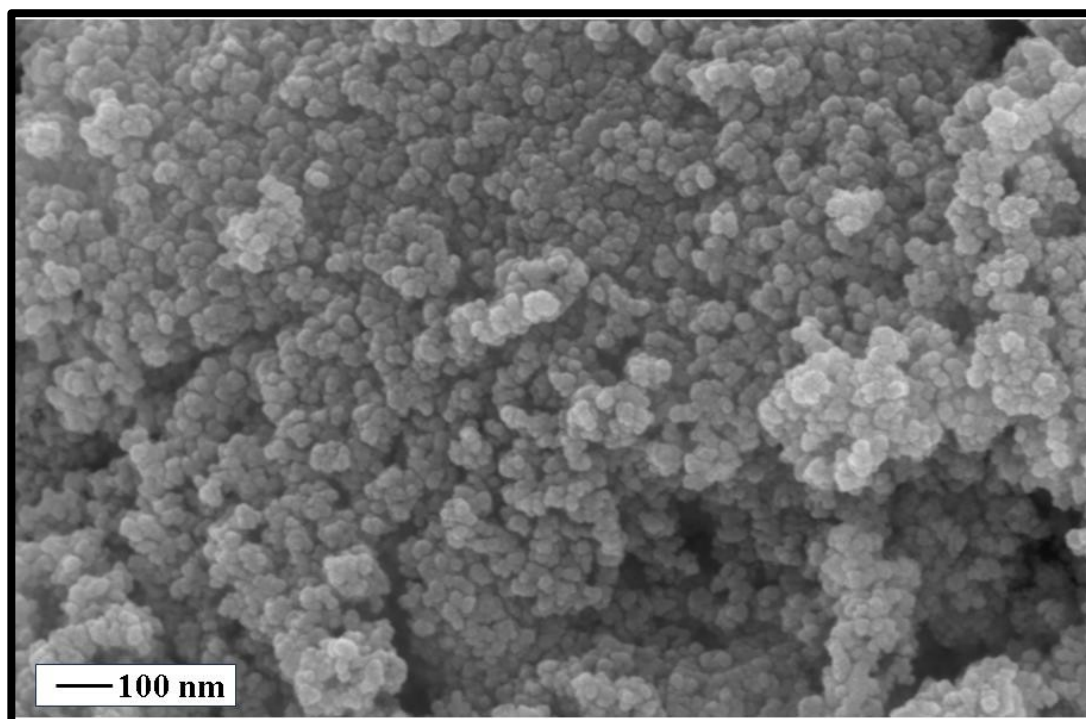
**Figure 3.3 FESEM of V$_2$O$_5$ nanoparticles**

## 3.3 Raman spectroscopy of V$_2$O$_5$: -

The vibrational modes inside the sample were found using Raman spectroscopy examination of the V$_2$O$_5$ NPs, as shown in Figure 3.4. The spectra show that α–V$_2$O$_5$ specific Raman-active modes are present. At 991 cm$^{-1}$, the maximum intensity Raman peak mode corresponding to V=O, is seen. This is explained by the displacement of O atoms by double bonds. At 137 cm$^{-1}$, bend vibrations at B$_{3g}$ were detected, and further low-frequency unique peaks at 188 cm$^{-1}$ were attributed to the O–V–O bending vibration modes [9] [26].
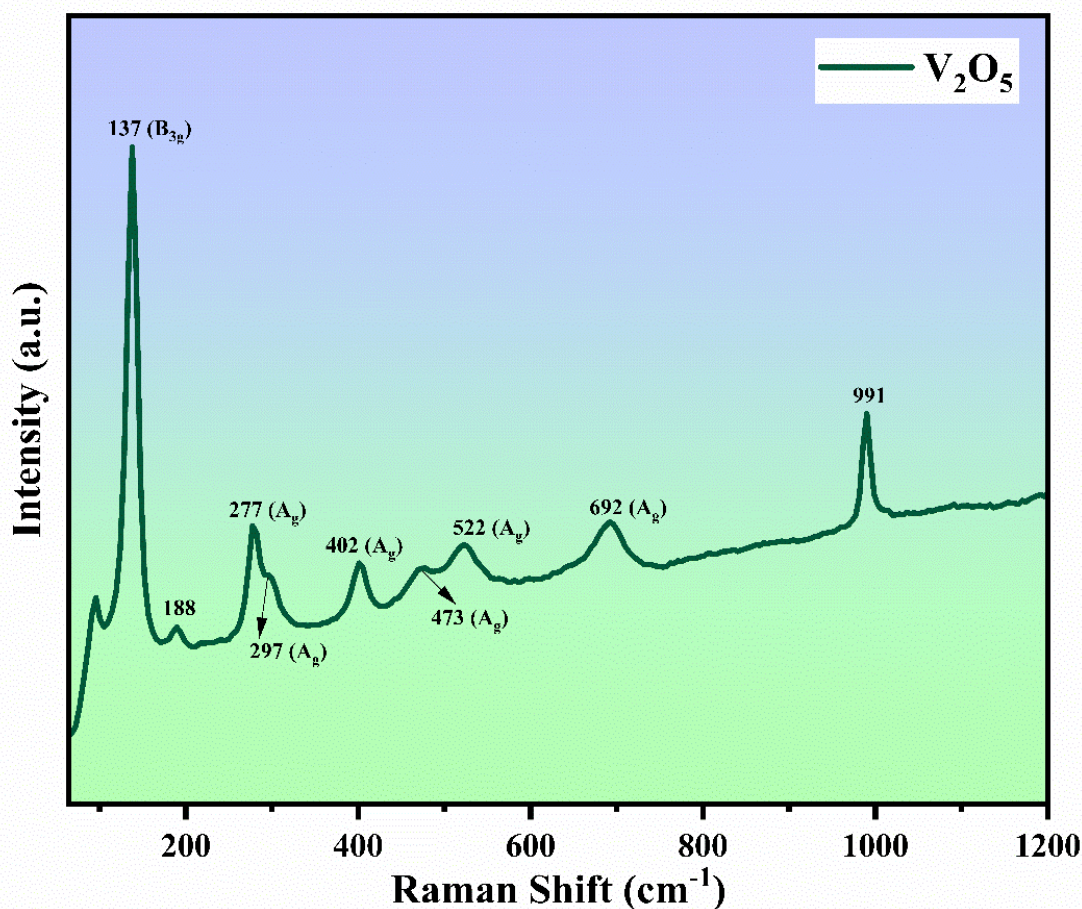
**Figure 3.4 Room temperature Raman spectra of $V_2O_5$ nanoparticles**

Furthermore, at V=O peaks, the $A_g$ mode of oscillating atoms was seen at 277 cm$^{-1}$, 297 cm$^{-1}$, & 402 cm$^{-1}$. In contrast, high-intensity peaks were found at 473 cm$^{-1}$, 522 cm$^{-1}$, & 692 cm$^{-1}$, respectively, in the vibration modes of $A_g$ [27] [28].

## 3.4 FTIR spectroscopy of $V_2O_5$: -

The existence of functional groups & different interactions within the 410–4000 cm$^{-1}$ range of $V_2O_5$ NPs were investigated using FTIR absorption spectra in combination with KBr medium. As shown in Figure 3.5, 3 absorption bands were found in the 450–1200 cm$^{-1}$ frequency range [21]. Double coordinated O vibrations (V–O–V) are associated with the lower frequency peak at 829 cm$^{-1}$ whereas stretching vibrations of terminal O bonds (V=O) are connected with the significantly higher frequency peak at 1013 cm$^{-1}$. Besides, V–O stretching correlates with the peak at 613 cm$^{-1}$ [29] [30].
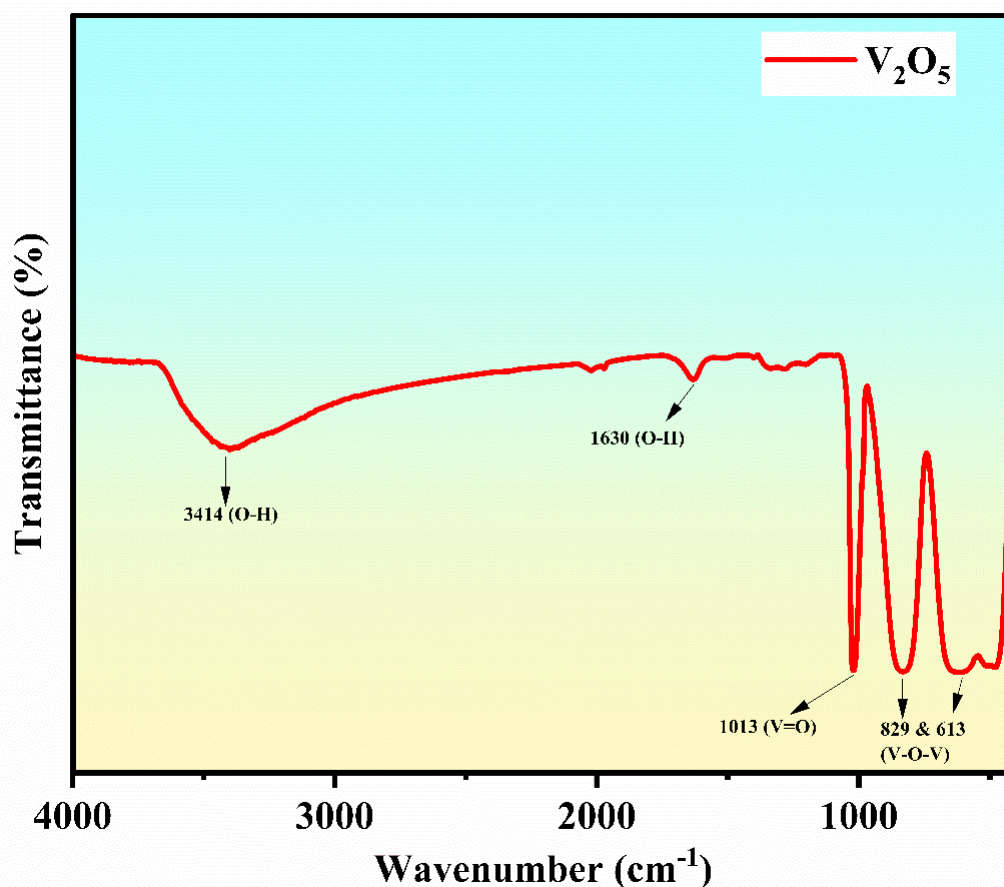
**Figure 3.5 FTIR of V₂O₅ nanoparticles**

Higher frequencies between 1600 & 3500 cm$^{-1}$ were where vibrations linked to water molecule adsorption were found. In particular, the band at 3414 cm$^{-1}$ indicates the stretching vibrations of water molecules adsorbed onto the surface, whereas the band at 1630 cm$^{-1}$ indicates the bend vibrations of adsorbed water molecules [31] [32].

## 3.5 PL spectroscopy of V₂O₅: -

One of the most remarkable features of semiconductors is their luminescence. Electrons move from the valence band to the conduction band when exposed to light that has a wavelength that is equal to or less than the absorption onset. Photons are released as the system relaxes [33]. PL examination was performed on the produced sample to verify the existence of O vacancies on the surface. Using an excitation wavelength of 325 nm, emission spectra in the 340–640 nm range were acquired

during PL observations of $V_2O_5$ NPs [34]. The PL spectrum of $V_2O_5$ NPs is shown in Figure 3.6. It shows a clear green emission peak at 539 nm, along with 2 other peaks at 413 nm & 468 nm, respectively, in the violet-blue emission area.
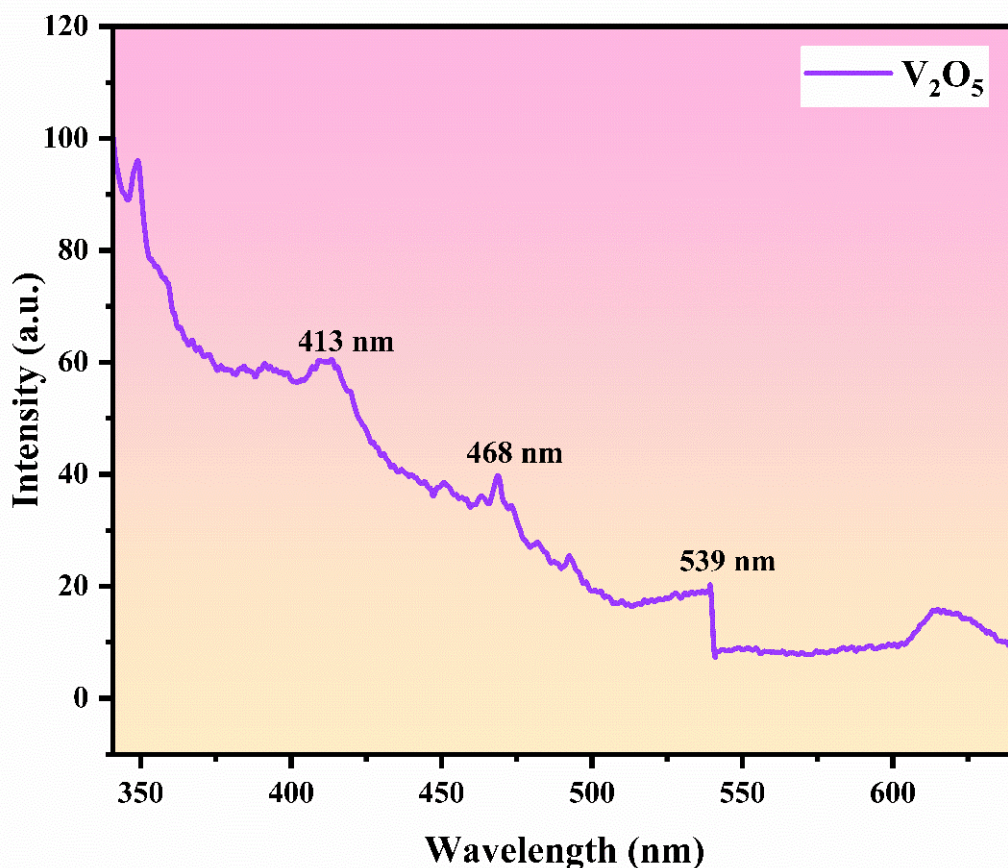


**Figure 3.6 PL spectra of $V_2O_5$ nanoparticles**

Transitions between the valence & conduction bands are shown by the green emission peak, which is correlated with V vacancies [21]. In the meanwhile, the emission peak at 413 nm results from the transition between the valence band & the V interstitial energy level. In addition, the as-prepared $V_2O_5$ NPs exhibit a greater electron concentration & a constant green light emission at room temperature, indicating their possible use in solar cells and light-emitting diodes [35].

## 3.6 BET analysis of $V_2O_5$: -

The BJH-derived distribution of the pore size v/s pore volume of $V_2O_5$ NPs is shown in Figure 3.7. The porosity & surface area of the material were determined using the BET model.
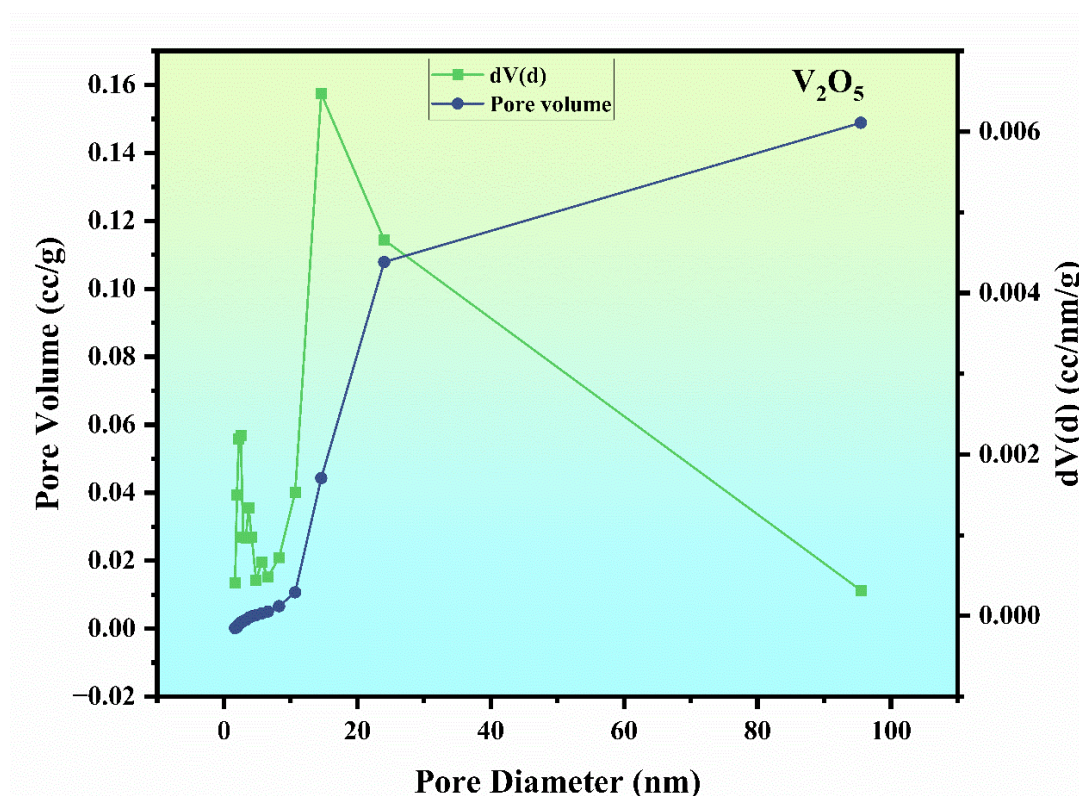


**Figure 3.7 BJH Pore size v/s pore volume distribution of $V_2O_5$ nanoparticles**

We have determined the adsorption-desorption isotherms with $N_2$ gas as the probing gas. The $N_2$ adsorption-desorption isothermal curve in Figure 3.8, in accordance with the IUPAC convention depicted a type V isotherm that followed the H1 type hysteresis loop for $V_2O_5$.
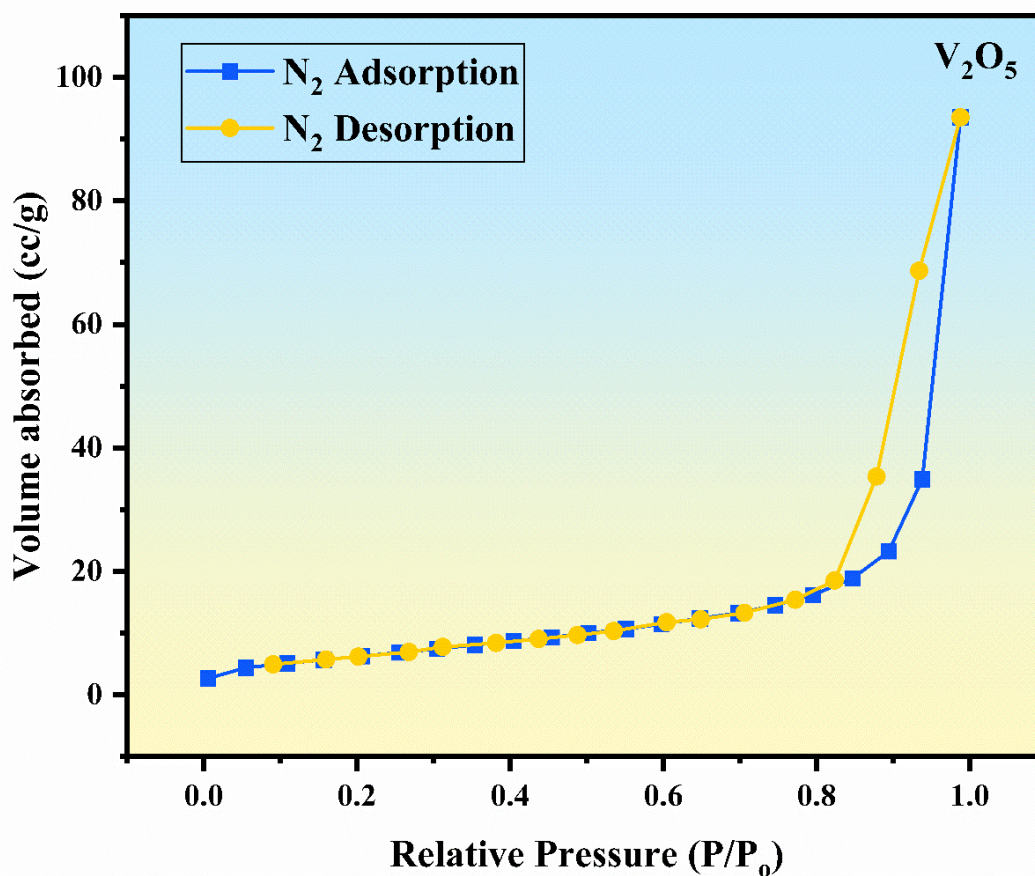
**Figure 3.8 Nitrogen adsorption-desorption isotherm of $V_2O_5$ nanoparticles**

The type V isotherm is distinguished by its hysteresis loop, which is linked to weak adsorbate-adsorbent interactions at low relative pressure & capillary condensation in mesopores [40] [41]. Mesoporous size distribution was observed in $V_2O_5$. The cumulative pore volume for $V_2O_5$ is determined to be 0.156 $cm^3g^{-1}$ at a relative pressure of $(P/P_o)$ for pores with a radius of less than 13.56 nm. Specific surface area of $V_2O_5$ is calculated to be 23.89 $m^2g^{-1}$ via the multipoint BET method [42] [43] [25].

## 3.7 EIS of $V_2O_5$: -

The Nyquist impedance response in an HEC provides information on the charge transfer mechanism, which is better understood with the use of EIS. The Nyquist curve offers unambiguous information on the ion diffusion that takes place in an HEC. The $V_2O_5$ HEC's wet state Nyquist curve is displayed in Figure 3.9, & the Nyquist plot is

used to compare the imaginary & real components of impedance in terms of frequency [44] [45].
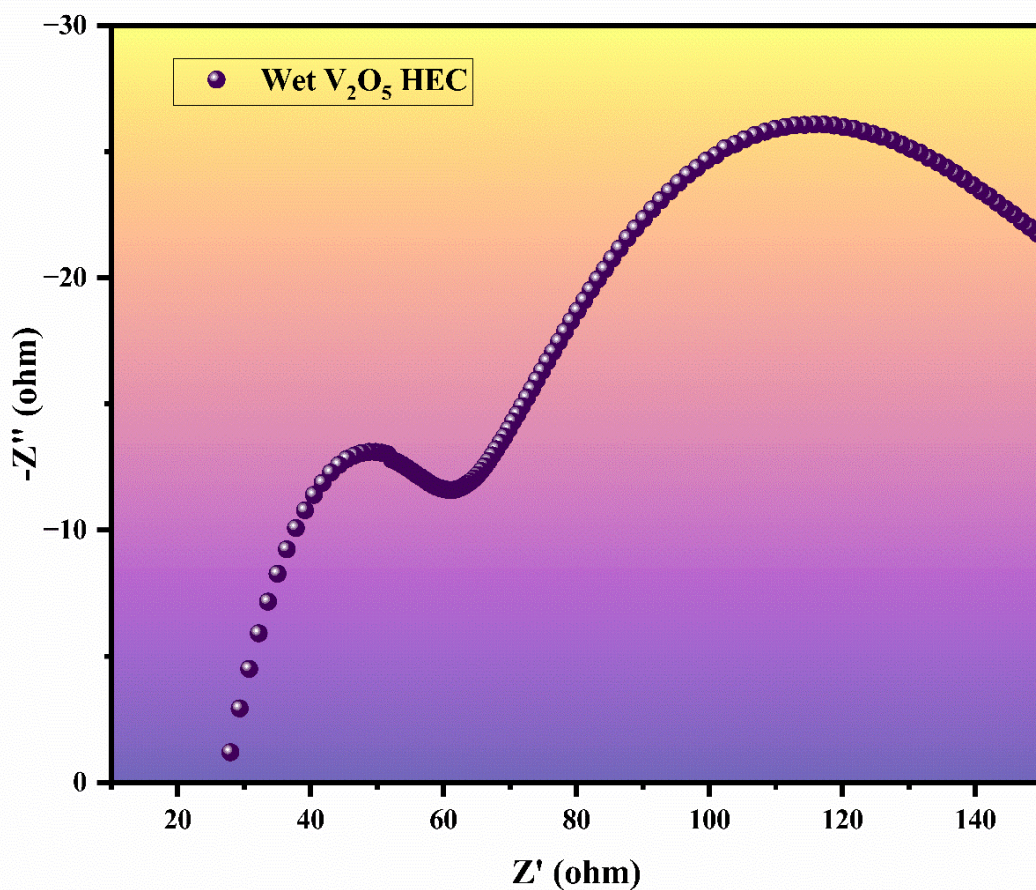


**Figure 3.9 Nyquist plot of V₂O₅ HEC in wet condition**

When the $V_2O_5$ HEC cell is wet, its resistance curve shows an extraordinarily high value of around $10^6$ $\Omega$. The resistance of HEC has been established by the semicircular fitting of the resultant Nyquist curve [34] [36]. The semicircle displays the $R_{ct}$ in the higher frequency range, while the interception of the impedance on the Z-real axis indicates the $R_s$ of the electrodes & electrolyte. Moreover, the produced $V_2O_5$ NP's sloping tail in the low-frequency region demonstrated enhanced capacitance behavior & ion diffusion at the electrode interface [46] [47].

# CHAPTER 4

# Hydroelectric Cell

## 4.1 Hydroelectric Properties: -

Small power generators called hydroelectric cells mostly produce energy from water. These are, to put it simply, water-activated cells. Low voltage, water activation, & environmental friendliness are a few of the fundamental characteristics of hydroelectric cells. The chemical reaction inside the cell that produces electricity is sparked by adding water as an activation agent. Because of the low voltage generated, this method is perfect for small-scale applications such as powering calculators and toys. HEC uses the water-splitting process to change water molecules into hydroxide & hydrogen ions. Unlike conventional batteries, HECs don't need an extra electrolyte, which makes it possible to produce green energy more sustainable & raises the cell's efficiency.

## 4.2 Water-Splitting Method: -

The hydroelectric cell's water-splitting mechanism is a basic electrochemical reaction that powers the production of clean, sustainable electricity, also known as water electrolysis. In this process, electrical energy is used to breakdown water molecules into hydrogen and oxygen.

Two half reactions are:

1. Oxidation at the anode:

   $2H_2O \rightarrow O_2 + 4H^+ + 4e^-$
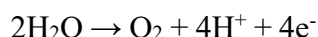
2. Reduction at the cathode:

   $4H^+ + 4e^- \rightarrow 2H_2$
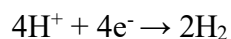
The overall equation is:

$2H_2O \rightarrow O_2 + 2H_2$

This reaction takes place at the anode & cathode of a hydropower cell & is fuelled by electrical energy. The oxygen gas produced at the anode is a valuable byproduct, while the hydrogen gas produced at the cathode may be used as a clean fuel source.

One of the main areas of research & development for renewable energy technologies is the efficiency & scalability of this water-splitting process. The full potential of this exciting electrochemical route may be realized by optimizing the catalysts, battery & operating parameters.
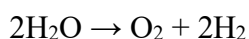
## 4.3 Working Mechanism: -

The two primary processes that drive the operation of an HEC are ionic conduction and the room-temperature adsorption of water molecules on the surface of $V_2O_5$ [48]. With its nanoporous structure and unsaturated oxygen-deficient surface covered with Ag in a grid pattern on one side, the specially-made $V_2O_5$ hydropower square pellet functions as an inert cathode, while the Zn sheet connected on the other side functions as an anode [49]. At room temperature, a few drops of DI water were put on the pellet surface, divided the water molecule into $OH^-$ & $H_3O^+$ ions [50]. While the hydronium ions hop to the Ag cathode, which absorbs electrons from the anode, the hydroxide ions migrate toward the Zn anode, releasing 2 electrons [51]. Diffusion across surfaces & capillaries is how these ions travel. Water molecules split at the oxygen vacancies & on the unsaturated cations that are present on the surface of $V_2O_5$ [36]. Since electrons are stuck at these oxygen vacancies, these vacancies function as hanging bonds. The water molecules are drawn to the trapped electrons, & the charged vacancies and coulombic attraction between surface cations weaken the O–H bond in the molecules.
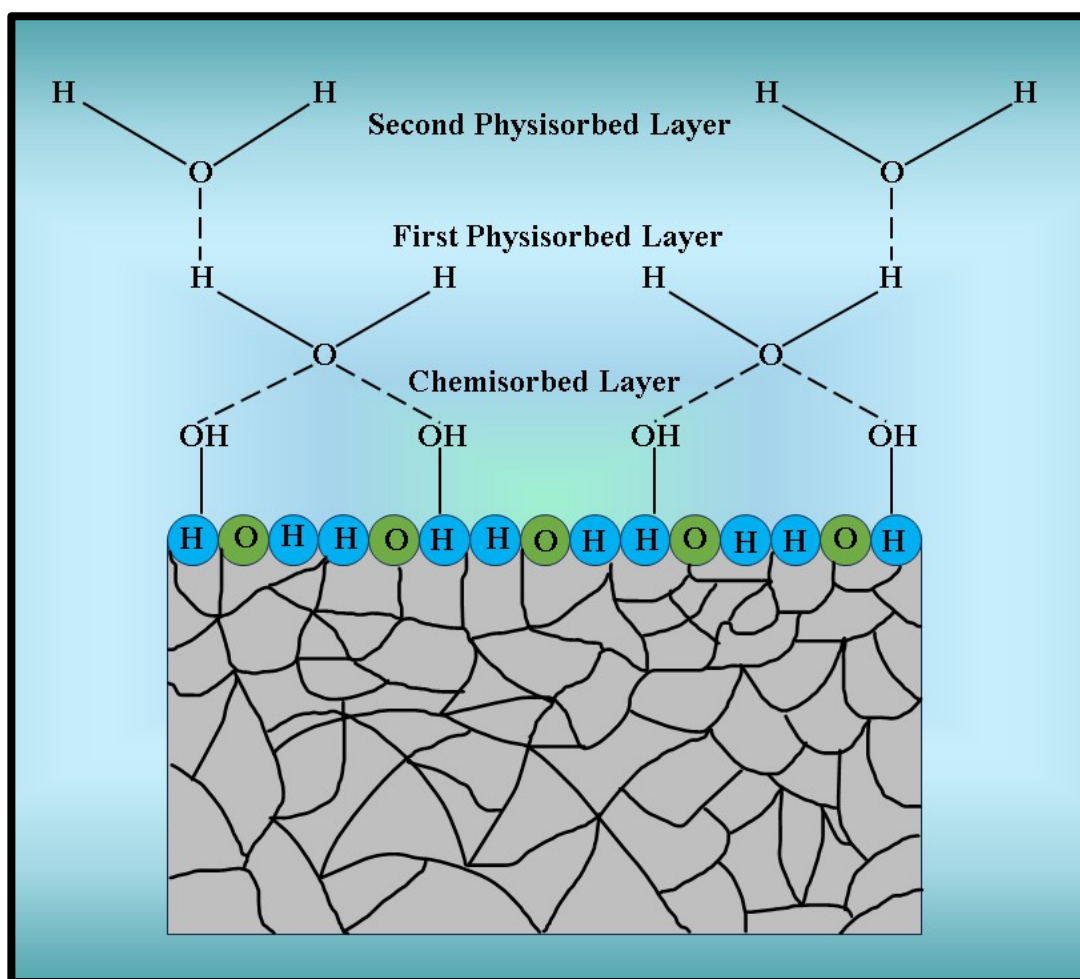
**Figure 4.1 Dissociation of water molecules on the surface of HEC**

Now, the unsaturated cation surface splits the OH⁻ ions, drawing them out and leaving behind $H_3O^+$ ions. Due to the confinement of these $H_3O^+$ ions in the $V_2O_5$ HEC nanopores, a strong EF is formed inside the pores. Further spontaneous dissociation of water molecules takes place on the surface due to the strong EF. An electrolytic or Groutthus chain reaction forms the OH⁻ layer, which is created by chemidissociation and the subsequent hopping of $H^+$ ions for conduction [51]. The splitting of water molecules caused by the generation of potential differences throughout the sample results in an EF, which is controlled by the subsequent electrochemical reaction process at the appropriate electrodes [52].
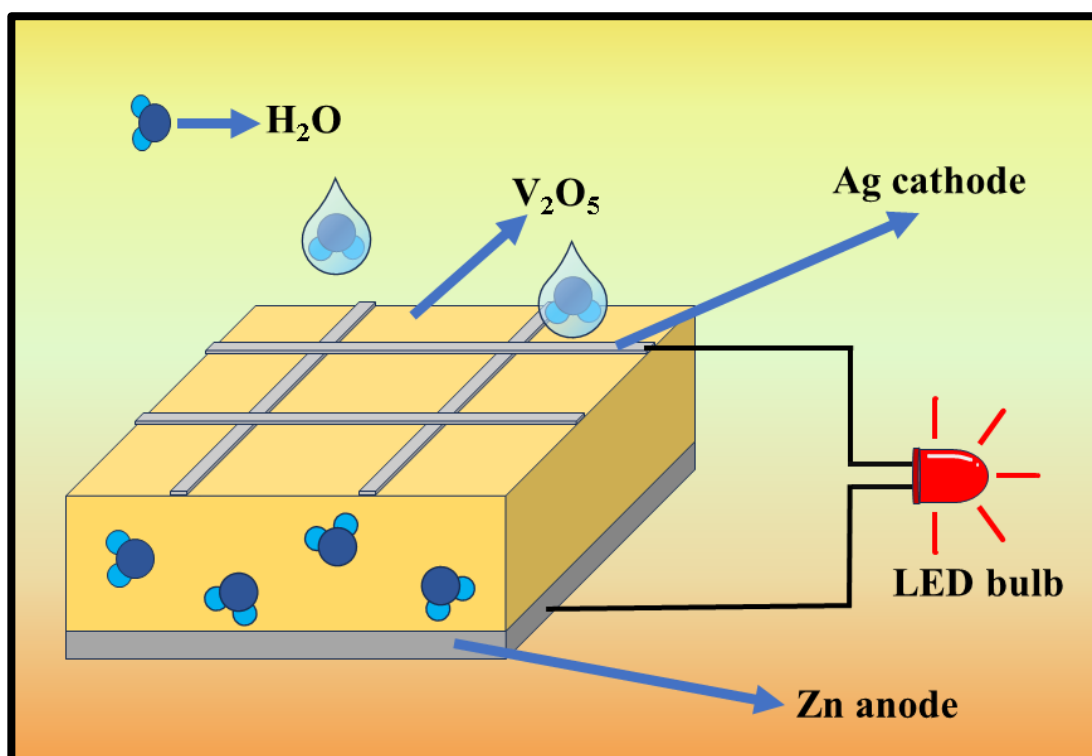
**Figure 4.2 Schematic diagram of working of $V_2O_5$ HEC**

Dissociation on surface defects of the HEC:

$$4H_2O \rightarrow 2OH^- + 2H_3O^+$$

Oxidation at the Zn anode:

$$Zn + 2OH^- \rightarrow Zn\,(OH)_2 + 2e^-$$
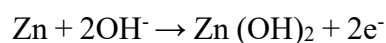
$$E_{oxd} = -0.76V$$

Reduction at Ag cathode along with $H_2$ gas liberation:

$$2H_3O^+ + 2e^- \rightarrow H_2(g) + 2H_2O$$
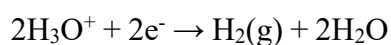
$$E_{red} = 0.22V$$

$E_{cell} = 0.98$ V is the net voltage produced by the electrodes. Voltage & current are produced in the cell by this ongoing redox reaction between the electrodes.

## 4.4 I-V Polarization: -

The effect of defect enhancement on water molecule splitting & the resulting production of ionic current is examined using the I-V polarization plot of the $V_2O_5$ HEC.

24
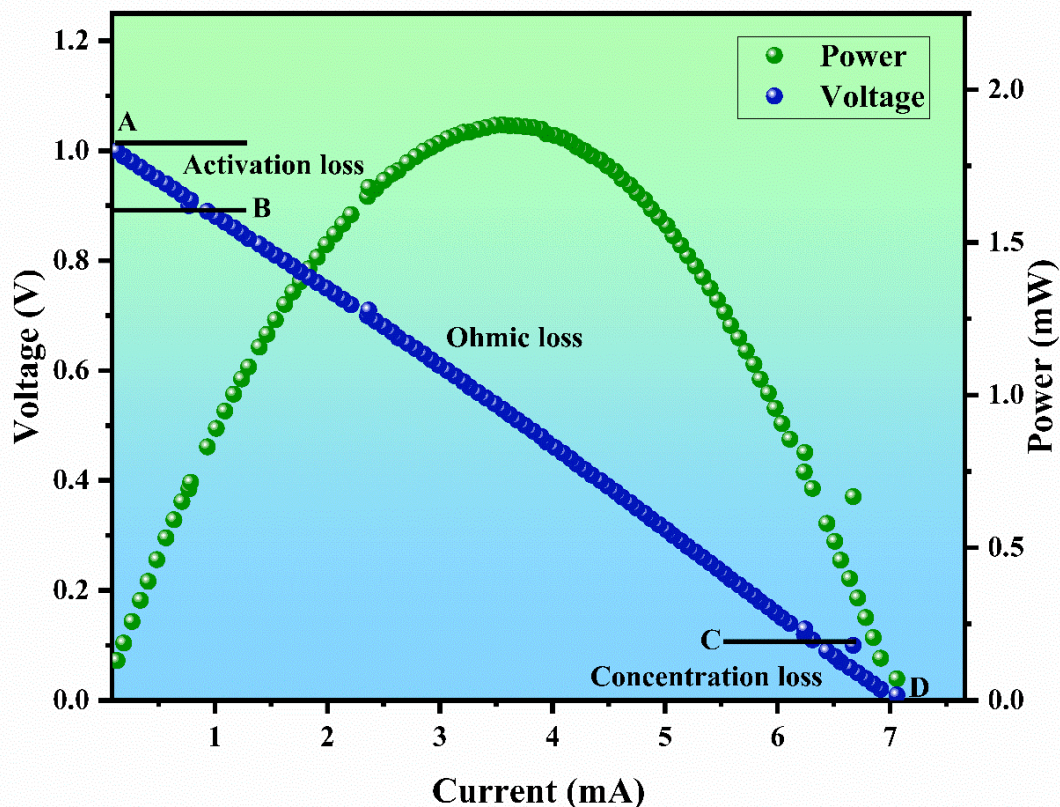
**Figure 4.3 I-V Polarization curve and energy generated by $V_2O_5$ HEC dipped in DI water**

After submerging the $V_2O_5$ pellet in DI water, the generated voltage & current were measured and plotted. The $V_2O_5$-based HEC produced maximum $I_{sc}$ ~ 7.06 mA. When both electrodes prevail equilibrium & there is no current flow in the cell, the voltage generated by the HEC is described by the maximum $V_{oc}$ ~ 1 V measured at point A as shown in Figure 4.3. Based on the acquired data, 7.06 mW is the maximum power of the manufactured HEC [54].

Three distinct zones have been seen in the I-V polarization curves of electrochemical cells:

 (i)  The activation loss region (AB region), also known as the low current density region, where the voltage rapidly declines. The primary reason it occurs is that in order to start the electrochemical reaction at the electrodes, some activation energy must be used to cross the energy barrier.

(ii)    The linear zone is represented by the ohmic loss region (BC region), also known as the moderate current density region, which is in charge of stopping the ionic flow. This loss results from the resistance that ions encounter when they travel through the material's porous surface & gather at the electrodes.

(iii)    The mass concentration loss region (CD region), also known as the high current density region, results in a sudden decrease in voltage with current because of the buildup of ions on the electrode surface; in other words, concentration loss occurs when there is not enough ion available for the electrodes during the hyperactive state.

Ultimately, these sections elucidate the kinetics of the electrochemical cell process [52] [53]. Thus, the net output voltage of the $V_2O_5$ based HEC is determined by:

$$V_{out} = E_{open\ cell} - V_{activation} - V_{ohmic} - V_{concentration}$$

Where open cell voltage is $E_{open\ cell}$ and $V_{activation}$, $V_{ohmic}$, and $V_{concentration}$ are overvoltage losses.

## 4.5 Water consumption in HEC

Charge of an electron, $e = 1.6 \times 10^{-19}$ C.

1 C $= 6.242 \times 10^{18}$ electrons.

1 ampere $= 6.242 \times 10^{18}$ electrons per second.

In 15.3mA, the number of electrons per second, n would be equal to,

$$15.3 \times 10^{-3} \times 6.242 \times 10^{18} = 95.502 \times 10^{15}$$

Open circuit voltage of the cell $= 0.98$V

One mole of electrons is equivalent to 96,485C/mole

So, the charge transfer in 15.3 mA $= e \times n$

$$= 1.6 \times 10^{-19} \times 95.502 \times 10^{15}$$
$$= 15.280 \times 10^{-3} \text{ C}$$

Hence, the number of moles will be $= 15.280 \times 10^{-3} / 96485$

$$= 1.583 \times 10^{-7} \text{mole}$$

We know, one mole contains 18mL of water.

So, quantity of water(mL) dissociating $= 18 \times 1.583 \times 10^{-7}$ mL

$$= 2.849 \text{ x } 10^{-6} \text{mL}$$

$$= 2.85 \mu \text{mL}$$

Therefore, 2.85μmL of water is required to generate 15.3 mA current for 1 second.

# CHAPTER 5

# Conclusion

Vanadium pentoxide nanoparticles ($V_2O_5$ NPs) were successfully and precisely synthesized using the solid-state sintering process. Comprehensive analyses using X-ray diffraction (XRD) and Raman spectroscopy confirmed that the synthesized sample possessed an orthorhombic structure with a dominant α- $V_2O_5$ phase. The sample exhibited enhanced crystallinity, with an average crystallite size measured at 22.81 nm. Further, field emission scanning electron microscopy (FESEM) scans revealed an average grain diameter of 81.6 nm, which corroborated our findings regarding the crystallinity and structural integrity of the $V_2O_5$ NPs.

Fourier-transform infrared (FTIR) spectroscopy provided additional insights, showing distinctive peaks indicative of stretching vibrations between vanadium (V) and oxygen (O) atoms in the $V_2O_5$ nanoparticles. These vibrations are characteristic of the $V_2O_5$ molecular structure, further validating the successful synthesis of high-purity $V_2O_5$ NPs.

Interestingly, photoluminescence (PL) measurements revealed significant changes in the oxidation states of the $V_2O_5$ nanoparticles. This observation suggests the presence of various oxidation states within the $V_2O_5$ lattice, which can influence the material's electronic and optical properties, making it potentially useful for various applications in electronics and photonics.

Additionally, the specific surface area of the synthesized $V_2O_5$ NPs was calculated to be 23.89 m²/g. This relatively high surface area is advantageous for applications requiring extensive surface interactions, such as catalysis, sensing, and energy storage. The electrical performance of the $V_2O_5$ NPs was also evaluated, revealing a maximum electric current of 7.06 mA and an output power of 7.06 mW. These findings highlight the potential of $V_2O_5$ NPs in electronic applications where efficient electrical conductivity is essential.

The cost-effectiveness of synthesizing $V_2O_5$ NPs through the solid-state sintering process, combined with their environmentally friendly nature, presents a viable option for the fabrication of hybrid energy cells (HECs). This synthesis method not only reduces production costs but also minimizes environmental impact, aligning with the growing demand for sustainable and green energy solutions.

Overall, the successful synthesis and comprehensive characterization of $V_2O_5$ nanoparticles underscore their potential in various technological applications. The orthorhombic structure with a dominant $\alpha$-$V_2O_5$ phase, high crystallinity, and substantial surface area make these nanoparticles suitable for use in green energy generation and storage devices. Their electrical properties, coupled with the ability to undergo significant changes in oxidation states, further expand their applicability in advanced electronic and optoelectronic devices.

The study highlights the potential of $V_2O_5$ NPs in contributing to clean energy solutions. Their synthesis is not only cost-effective but also aligns with environmental sustainability goals, making them an attractive option for the development of hybrid energy cells. The detailed structural, optical, and electrical characterizations provide a strong foundation for future research and development in this field, paving the way for innovative applications in green energy and beyond.

In conclusion, the precise synthesis and thorough characterization of $V_2O_5$ nanoparticles demonstrate their significant potential in various high-tech applications. Their unique properties, combined with cost-effective and environmentally friendly production methods, make them an excellent candidate for advancing green energy technologies. This research paves the way for future innovations that leverage the exceptional qualities of $V_2O_5$ NPs for sustainable and efficient energy solutions.

# REFERENCES

[1] Le, Top Khac, Manil Kang, and Sok Won Kim. "Room-temperature photoluminescence behaviour of α-V2O5 and mixed α-β phase V2O5 films grown by electrodeposition." *Materials Science in Semiconductor Processing* 94 (2019): 15-21.

[2] Le, Top Khac, Manil Kang, and Sok Won Kim. "A review on the optical characterization of V2O5 micro-nanostructures." Ceramics International 45, no. 13 (2019): 15781-15798.

[3] Basu, Raktima, and Sandip Dhara. "Spectroscopic study of native defects in the semiconductor to metal phase transition in V2O5 nanostructure." Journal of Applied Physics 123, no. 16 (2018).

[4] Le, Top Khac, Manil Kang, and Sok Won Kim. "Morphology engineering, room-temperature photoluminescence behavior, and sunlight photocatalytic activity of V2O5 nanostructures." Materials Characterization 153 (2019): 52-59.

[5] Li, Yanwei, Jinhuan Yao, Evan Uchaker, Ming Zhang, Jianjun Tian, Xiaoyan Liu, and Guozhong Cao. "Sn-doped V2O5 film with enhanced lithium-ion storage performance." The Journal of Physical Chemistry C 117, no. 45 (2013): 23507-23514.

[6] ] Hu, Peng, Ping Hu, Tuan Duc Vu, Ming Li, Shancheng Wang, Yujie Ke, Xianting Zeng, Liqiang Mai, and Yi Long. "Vanadium Oxide: Phase Diagrams, Structures, Synthesis, and Applications." Chemical Reviews 123, no. 8 (2023): 4353-4415.

[7] WookáHan, Sang, and Sok WonáKim. "Highly intense room-temperature photoluminescence in V 2 O 5 nanospheres." RSC advances 8, no. 72 (2018): 41317-41322.

[8] Hu, Yin, Zhengcao Li, Zhengjun Zhang, and Daqiao Meng. "Effect of magnetic field on the visible light emission of V2O5 nanorods." Applied Physics Letters 94, no. 10 (2009).

[9] Othonos, Andreas, Constantinos Christofides, and Matthew Zervos. "Ultrafast transient spectroscopy and photoluminescence properties of V2O5 nanowires." Applied Physics Letters 103, no. 13 (2013).

[10]      Zou, Chongwen, Lele Fan, Ruiqun Chen, Xiaodong Yan, Wensheng Yan, Guoqiang Pan, Ziyu Wu, and Wei Gao. "Thermally driven V 2 O 5 nanocrystal formation and the temperature-dependent electronic structure study." CrystEngComm 14, no. 2 (2012): 626-631.

[11]      Asadov, Alec, Surayya Mukhtar, and Wei Gao. "Crystal structure development of vanadium oxide thin films deposited by a magnetron sputtering technique." Journal of Vacuum Science & Technology B 33, no. 4 (2015).

[12]      Singh, Preetam, and Davinder Kaur. "Influence of film thickness on texture and electrical and optical properties of room temperature deposited nanocrystalline V2O5 thin films." Journal of Applied Physics 103, no. 4 (2008).

[13]      Zou, C. W., X. D. Yan, Darrell A. Patterson, Emma AC Emanuelsson, J. M. Bian, and W. Gao. "Temperature sensitive crystallization of V 2 O 5: from amorphous film to β-V 2 O 5 nanorods." CrystEngComm 12, no. 3 (2010): 691-693.

[14]      Natalio, Filipe, Rute André, Aloysius F. Hartog, Brigitte Stoll, Klaus Peter Jochum, Ron Wever, and Wolfgang Tremel. "Vanadium pentoxide nanoparticles mimic vanadium haloperoxidases and thwart biofilm formation." Nature nanotechnology 7, no. 8 (2012): 530-535.

[15]      Shafeeq, K. M., V. P. Athira, CH Raj Kishor, and P. M. Aneesh. "Structural and optical properties of V 2 O 5 nanostructures grown by thermal decomposition technique." Applied Physics A 126 (2020): 1-6.

[16]      Govindarajan, D., V. Uma Shankar, and R. Gopalakrishnan. "Supercapacitor behavior and characterization of RGO anchored V 2 O 5 nanorods." Journal of Materials Science: Materials in Electronics 30 (2019): 16142-16155.

[17]      Kosta, I., Ch Navone, A. Bianchin, E. García-Lecina, H. Grande, H. Ihou Mouko, J. Azpeitia, and I. García. "Influence of vanadium oxides

nanoparticles on thermoelectric properties of an N-type Mg2Si0. 888Sn0. 1Sb0. 012 alloy." Journal of Alloys and Compounds 856 (2021): 158069.

[18]     Mousavi, Maliheh, Shekoofeh Tabatabai Yazdi, and GholamHossein Khorrami. "Structural, Optical and Magnetic Characterization of Vanadium Pentoxide Nanoparticles Synthesized in a Gelatin Medium." Journal of Nanostructures 11, no. 1 (2021): 105-113.

[19]     Hassan, Zahra A., and Rashed T. Rasheed. "Preparation of V2O5 and SnO2 Nanoparticles and their application as pollutant removal." Journal of Applied Sciences and Nanotechnology 1, no. 4 (2021): 69-80.

[20]     Saini, Sandeep, Jyoti Shah, R. K. Kotnala, and K. L. Yadav. "Nickel substituted oxygen deficient nanoporous lithium ferrite based green energy device hydroelectric cell." Journal of alloys and compounds 827 (2020): 154334.

[21]     Prześniak-Welenc, Marta, M. Łapiński, Tomasz Lewandowski, Barbara Kościelska, Leszek Wicikowski, and Wojciech Sadowski. "The influence of thermal conditions on V2O5 nanostructures prepared by sol-gel method." Journal of Nanomaterials 2015 (2015): 3-3.

[22]     Sobhani, Azam, and Masoud Salavati-Niasari. "A new simple route for the preparation of nanosized copper selenides under different conditions." Ceramics International 40, no. 6 (2014): 8173-8182.

[23]     Abd-Alghafour, N. M., Naser M. Ahmed, Z. Hassan, Sabah M. Mohammad, M. Bououdina, and Mohammed KM Ali. "Characterization of V 2 O 5 nanorods grown by spray pyrolysis technique." Journal of Materials Science: Materials in Electronics 27 (2016): 4613-4621.

[24]     Abd-Alghafour, N. M., Naser M. Ahmed, Z. Hassan, and M. Bououdina. "High-performance p–n heterojunction photodetectors based on V 2 O 5 nanorods by spray pyrolysis." Applied Physics A 122 (2016): 1-9.

[25]     Ibrahim, Y., A. B. Kashyout, I. Morsi, and H. Shokry Hassan. "Development of nano-SnO2 and SnO2: V2O5 thin films for selective gas sensor devices." Arabian Journal for Science and Engineering 46, no. 1 (2021): 669-686.

[26]     Abd-Alghafour, N. M., Naser M. Ahmed, Z. Hassan, and Munirah Abdullah Almessiere. "Hydrothermal synthesis and structural properties of V2O5 nanoflowers at low temperatures." In Journal of Physics: Conference Series, vol. 1083, no. 1, p. 012036. IOP Publishing, 2018.

[27]     Zheng, Chenmou, Xinmin Zhang, Zhengping Qiao, and Deming Lei. "Preparation and characterization of nanocrystal V2O5." Journal of Solid State Chemistry 159, no. 1 (2001): 181-185.

[28]     Thakur, Yugesh Singh, Aman Deep Acharya, Sakshi Sharma, and Sagar Bisoyi. "Enhanced electrochemical performance of in situ polymerized V2O5-PANI nanocomposites and its practical application confirmation by assembling ionic liquid as well as solid state-based supercapacitor device." Results in Chemistry 7 (2024): 101259.

[29]     Alghool, Samir, Hanan F. Abd El-Halim, and Ayman M. Mostafa. "An eco-friendly synthesis of V2O5 nanoparticles and their catalytic activity for the degradation of 4-nitrophrnol." Journal of Inorganic and Organometallic Polymers and Materials 29, no. 4 (2019): 1324-1330.

[30]     Chen, Yu, Cheng Chen, Wei Chen, Heng Liu, and Jianguo Zhu. "Influence of thermal-decomposition temperatures on structures and properties of V2O5 as cathode materials for lithium ion battery." Progress in Natural Science: Materials International 25, no. 1 (2015): 42-46.

[31]     Wang, Chiyuan, Huiyan Xu, Tongyao Liu, Shuaijun Yang, Yong Nie, Cheng Wang, Xiaodan Guo, Binbin Wang, Xin Ma, and Xuchuan Jiang. "One- step ball milling synthesis of VO 2 (M) nanoparticles with exemplary thermochromic performance." SN Applied Sciences 3 (2021): 1-10.

[32]     Abd-Alghafour, N. M., Naser M. Ahmed, and Zainuriah Hassan. "Fabrication and characterization of V2O5 nanorods based metal– semiconductor–metal photodetector." Sensors and Actuators A: Physical 250 (2016): 250-257.

[33]     Rosaiah, P., G. Lakshmi Sandhya, and O. M. Hussain. "Impedance spectroscopy and electrochemical properties of nano-crystalline vanadium pentoxide (V2O5) synthesized by co-precipitation method." Advanced Science, Engineering and Medicine 8, no. 2 (2016): 83-90.

[34]      Surya Bhaskaram, D., Rajesh Cheruku, and G. Govindaraj. "Reduced graphene oxide wrapped V 2 O 5 nanoparticles: green synthesis and electrical properties." Journal of Materials Science: Materials in Electronics 27 (2016): 10855-10863.

[35]      Molli, Muralikrishna, Abhijit Bhat Kademane, Prabin Pradhan, and V. Sai Muthukumar. "Study of nonlinear optical absorption properties of V 2 O 5 nanoparticles in the femtosecond excitation regime." Applied physics A 122 (2016): 1-4.

[36]      Gaur, Anurag, Anurag Kumar, Purushottam Kumar, Rekha Agrawal, Jyoti Shah, and Ravinder K. Kotnala. "Fabrication of a SnO2-based hydroelectric cell for green energy production." ACS omega 5, no. 18 (2020): 10240-10246.

[37]      Das, Rojaleena, Jyoti Shah, Sanjeev Sharma, Pritam Babu Sharma, and Ravinder Kumar Kotnala. "Electricity generation by splitting of water from hydroelectric cell: an alternative to solar cell and fuel cell." International Journal of Energy Research 44, no. 14 (2020): 11111-11134.

[38]      Kumar, Parveen, Shruti Vashishth, Isha Sharma, and Vivek Verma. "Porous SnO2 ceramic-based hydroelectric cells for green power generation." Journal of Materials Science: Materials in Electronics 32, no. 1 (2021): 1052-1060.

[39]      Kotnala, R. K., Rekha Gupta, Abha Shukla, Shipra Jain, Anurag Gaur, and Jyoti Shah. "Metal oxide based hydroelectric cell for electricity generation by water molecule dissociation without electrolyte/acid." The Journal of Physical Chemistry C 122, no. 33 (2018): 18841-18849.

[40]      Zhang, Pengfei. "Adsorption and desorption isotherms." KE group (2016).

[41]      Sing, Kenneth SW, and Ruth T. Williams. "Physisorption hysteresis loops and the characterization of nanoporous materials." Adsorption Science & Technology 22, no. 10 (2004): 773-782.

[42]      Saini, Anmol, Rajiv Kashyap, Jyoti Rani, and Ramesh K. Sharma. "Electrical energy of the order of 24 W/m2 from water splitting using nickel

oxide: effect of synthesis process on power output." Results in Chemistry 5 (2023): 100911.

[43]     Ng, See How, Sau Yen Chew, Jiazhao Wang, David Wexler, Y. Tournayre, K. Konstantinov, and Hua-Kun Liu. "Synthesis and electrochemical properties of V2O5 nanostructures prepared via a precipitation process for lithium-ion battery cathodes." Journal of Power Sources 174, no. 2 (2007): 1032-1035.

[44]     Dhananjaya, M., N. Guru Prakash, A. Lakshmi Narayana, and O. M. Hussain. "Microstructural and supercapacitive properties of one-dimensional vanadium pentoxide nanowires synthesized by hydrothermal method." Applied Physics A 124 (2018): 1-7.

[45]     Sarwar, Zartasha, Muhammad Umair, Yasir Javed, S. Hussain, Naveed Akhtar Shad, Asim Jilani, Aqeel Ahmed Shah, Muhammad Azam, and Sumara Ashraf. "Effect of cerium oxide and rGO conjugation on the electrochemical energy storage traits of V2O5 nanomaterials." Journal of Electronic Materials 52, no. 10 (2023): 6578-6593.

[46]     Sutrave, Shivani, Shireesha Konda, Divya Velpula, Sriram Ankith Volety, Sugunakar Reddy Ravula, Shilpa Chakra Chidurala, and Bala Narsaiah Tumma. "A simple solution combustion method for the synthesis of V2O5 nanostructures for supercapacitor applications." Applied Surface Science Advances 12 (2022): 100331.

[47]     Zhang, Yifu, Jiqi Zheng, Qiushi Wang, Shaoqing Zhang, Tao Hu, and Changgong Meng. "One-step hydrothermal preparation of (NH4) 2V3O8/carbon composites and conversion to porous V2O5 nanoparticles as supercapacitor electrode with excellent pseudocapacitive capability." Applied Surface Science 423 (2017): 728-742.

[48]     Kumar, Parveen, Neelam Singh, Pradumn Kumar, and Vivek Verma. "Nanocomposite based hydroelectric cells: Working principle and production of green electrical energy." Inorganic Chemistry Communications 141 (2022): 109515.

[49]     Bhargava, Richa, Jyoti Shah, Shakeel Khan, and R. K. Kotnala. "Hydroelectric cell based on a cerium oxide-decorated reduced graphene oxide

(CeO2–rG) nanocomposite generates green electricity by room-temperature water splitting." Energy & Fuels 34, no. 10 (2020): 13067-13078.

[50]     Gupta, Rekha, Jyoti Shah, Rojaleena Das, Sandeep Saini, and R. K. Kotnala. "Defect-mediated ionic hopping and green electricity generation in Al 2− x Mg x O 3-based hydroelectric cell." Journal of Materials Science 56 (2021): 1600-1611.

[51]     Jain, Shipra, Jyoti Shah, S. R. Dhakate, Govind Gupta, C. Sharma, and R. K. Kotnala. "Environment-friendly mesoporous magnetite nanoparticles-based hydroelectric cell." The Journal of Physical Chemistry C 122, no. 11 (2018): 5908-5916.

[52]     Saini, Sandeep, Kanhaiya L. Yadav, Jyoti Shah, and Ravinder K. Kotnala. "Effect of Li+, Mg2+, and Al3+ substitution on the performance of nickel ferrite-based hydroelectric cells." Energy & Fuels 36, no. 13 (2022): 7121-7129.

[53]     Saini, Sandeep, Jyoti Shah, R. K. Kotnala, and K. L. Yadav. "Nickel substituted oxygen deficient nanoporous lithium ferrite based green energy device hydroelectric cell." Journal of alloys and compounds 827 (2020): 154334.

[54]     Gupta, Rekha, Jyoti Shah, Rakesh Singh, and R. K. Kotnala. "Nonphotocatalytic water splitting process to generate green electricity in alkali doped zinc oxide based hydroelectric cell." Energy & Fuels 35, no. 11 (2021): 9714-9726.

# LIST OF PUBLICATION & PROOF



ICAMNOP - 2023

International Conference on
Atomic, Molecular, Material, Nano, and Optical Physics with Applications

20th - 22nd December, 2023

Organized by:
Department of Applied Physics, Delhi Technological University, Delhi, India

## Certificate

This is to certify that

Prof./Dr./Mr./Ms. _____Archana Krishnan_____

has presented Poster / Oral Presentation in the "International Conference on Atomic, Molecular, Material, Nano and Optical Physics with Applications (ICAMNOP-2023)" held at Delhi Technological University, Delhi, India during 20th-22nd December, 2023.

Prof. Rinku Sharma
President, ICAMNOP-2023

Prof. A. S. Rao
Chairperson, ICAMNOP-2023

Prof. Vinod Singh
Convener, ICAMNOP-2023

SERB DIA          Ω Metrohm

# SCOPUS INDEX



Springer

Search    Authors & Editors    Account

Book series

## Springer Proceedings in Physics

### About this book series

Indexed by Scopus

The series Springer Proceedings in Physics, founded in 1984, is devoted to timely reports of state-of-the-art developments in physics and related sciences. Typically based on material presented at conferences, workshops and similar scientific meetings, volumes published in this series will constitute a comprehensive up to date source of reference on a field or subfield of relevance in contemporary physics. Proposals must include the following: — show all

**Electronic ISSN**     **Print ISSN**
1867-4941               0930-8989

### Book titles in this series

Proceedings of the 9th International Symposium on Hydrogen Energy, Renewable Energy and Materials
HEREM23, Oct. 13-14, 2023, Bangkok, Thailand

### Publish with us

Submission guidelines

Open access publishing

Policies and ethics

**Contact the Publishing Editor**
Zachary Evenson ✉

⬇ Download book proposal form



**International Conference on Atomic, Molecular, Material, Nano and Optical Physics with Applications (ICAMNOP–2023)**
Organized by: Department of Applied Physics, Delhi Technological University Delhi-110042, India
December 20th-22nd, 2023

HOME    CONFERENCE    COMMITTEE    SPEAKERS    PUBLICATION    REGISTRATION    ABSTRACTS    ACCOMMODATION    TOUR    GALLERY    CONTACT US

Login

### About The Conference

International Conference on Atomic, Molecular, Material, Nano and Optical Physics with Applications (ICAMNOP-2023) will focus on developments in atomic, molecular, material, Nano and Optical Physics which have proved to be powerful science supporting many other areas of science & technology, including industrial, information, energy, global Change, defense, health and medical environmental, space and transportation technology.

Read More »

# PLAGIARISM REPORT

PAPER NAME

**Archana thesis.docx**

| | |
|---|---|
| WORD COUNT | CHARACTER COUNT |
| **6897 Words** | **38445 Characters** |
| PAGE COUNT | FILE SIZE |
| **47 Pages** | **5.7MB** |
| SUBMISSION DATE | REPORT DATE |
| **Jun 4, 2024 1:30 AM GMT+5:30** | **Jun 4, 2024 1:31 AM GMT+5:30** |

● **5% Overall Similarity**

The combined total of all matches, including overlapping sources, for each database.

- 3% Internet database
- Crossref database
- 3% Submitted Works database
- 3% Publications database
- Crossref Posted Content database

● **Excluded from Similarity Report**

- Bibliographic material
- Cited material
- Quoted material
- Small Matches (Less then 10 words)